Hindawi Publishing Corporation
Mathematical Problems in Engineering
Volume 2015, Article ID 106159, 10 pages
http://dx.doi.org/10.1155/2015/106159

Research Article

Research on Stability Prediction of the Crankshaft CNC Tangential Point Tracing Grinding

Zhuoda Jiang[1,2] and Yongyi He[1]

[1] *Shanghai Key Laboratory of Intelligent Manufacturing and Robotics, School of Mechatronic Engineering and Automation, Shanghai University, No. 149 Yanchang Road, Mailbox 232, Shanghai 200072, China*
[2] *Jiangxi Key Laboratory of Numerical Control, Jiujiang University, Jiujiang, Jiangxi 332005, China*

Correspondence should be addressed to Zhuoda Jiang; jzd000@163.com

Received 16 June 2015; Revised 31 August 2015; Accepted 6 September 2015

Academic Editor: Ivanka Stamova

As the key part of internal combustion engines, crankshaft with high efficiency and accuracy processing has always been the target of the engine manufacturer's pursuit. Grinding is used to obtain the ultimate dimensional accuracy and surface finish in the crankshaft machining. Grinding of the main journals and the pin journals can be accomplished in a single clamping operation by CNC Tangential Point Tracing grinding technology. However, the chatter in the grinding process is harmful to the precision and surface quality. In this paper, stability lobe diagram is developed to predict the grinding chatter. First the dynamic model of Tangential Point Tracing grinding system is established. Then the limit formula of the critical grinding depth is calculated and the stability lobe diagram of the grinding system is presented. Finally, the validation experiments are carried out on the crankshaft grinding machine and the results are consistent with the calculation.

1. Introduction

Crankshaft is one of the key components of engines in automotive industry and its rotation is the power source of the engine. It consists of two important parts: the crankshaft main journal and crankpin. The crankshaft main journal is mounted on the cylinder, while the crankpin is connected to the big end hole of the connecting rod and its other end hole is connected to the cylinder piston. It is a typical slider crank mechanism and it turns the reciprocating motion of the connecting rod into rotating motion. The quality of crankshaft determines the performance of the engine. The crankshaft of an engine is shown in Figure 1.

The traditional crankshaft grinding process of main journal is similar to the cylindrical grinding. The crankpin is adjusted to the center of the grinding by the eccentric fixture and each crankshaft needs special fixture. It has long auxiliary hours and low processing precision when the clamp is adjusting by the operator [1].

Nowadays, the crankshaft is mechanized by the method of CNC Tangential Point Tracing grinding. Grinding of the main journals and the pin journals can be accomplished in a single clamping operation. The grinding method can avoid the positioning error caused by multiple loadings and save the adjustment time. High machining flexibility, accuracy, and efficiency are also improved. CNC Tangential Point Tracing Grinding Crankshaft is high technology processing and it was called Oscillate grinding [2] or Chasing the pin [3] by some scholars. Tangential Point Tracing grinding mode is composed of linkage between the workpiece rotation (C axis) and reciprocating motion of the grinding wheel (x axis) to achieve the eccentric circle machining.

The chatter in the grinding process can result in increased tolerance of dimension and position, the surface roughness and waviness, which seriously affect dimensional accuracy and surface finish of the crankshaft. The chatter in the machining is usually accompanied by considerable noise [4].

There are lots of measures that can effectively control chatter such as using the drive to improve the dynamic stiffness and damping of the grinding machine system to reduce the regenerative phase [5], but these methods need to change the structure of machine tools and they are *not* suitable for the users.

Figure 1: Crankshaft.

The stability of the stable region and the unstable region can be visually described by the stability lobe diagram [6, 7]. In order to avoid the grinding chatter, the Tangential Point Tracing grinding was set as the research object. The stability lobe chart was used to visually describe the grinding stability region and the unstable region. To predict the grinding stability, the machining quality and the machining efficiency of the grinding process are ensured [8].

2. The Tangential Point Tracing Grinding

With increased demands of industry, Tangential Point Tracing grinding process has been developed to machine non-round shaped parts such as crankshaft and camshaft allowing reduction of nonproductive time and reclamping inaccuracies [9].

The grinding point moves along the surface of the crankpin, while the grinding wheel is always tangent to the crankpin in the grinding process. Figure 2 illustrates the concept of Tangential Point Tracing grinding [3]. The crankpin rotates around the C axis followed by horizontal movement of the wheel head along the x axis. All of the main journals and crankpins of a concentrically clamped crankshaft can be machined in one fixture that improves the efficiency and accuracy of the products.

Figure 3 is the schematic of Tangential Point Tracing grinding motion model. The crankpin is rotated around the O point, and the wheel is followed by the movement. The trajectory equation of the tangent points coordinates can be expressed as follows:

$$\begin{aligned} x &= R\cos\alpha + R_W\cos\beta \\ y &= R\sin\alpha - R_W\sin\beta \\ R\sin\alpha &= (R_S + R_W)\sin\beta. \end{aligned} \tag{1}$$

In Figure 3, O is the crankshaft turning center. O_W denotes the center of the crankpin. O_S is the center of the grinding wheel.

The eccentric distance of the crankpin is R. R_W and R_S correspond to the radius of the crankpin and the grinding wheel, respectively.

Here, α and β denote the rotation angle of the crankshaft and the angle between $\overline{O_S O_W}$ and $\overline{OO_S}$.

x and y is describe the position of the tangent point T in rectangular coordinate system, where O is origin of coordinate system.

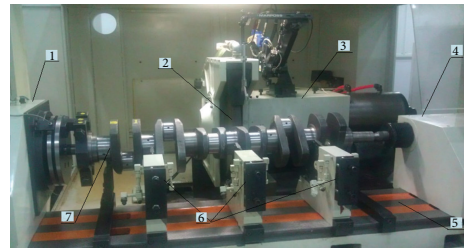

Figure 2: Tangential Point Tracing crankshaft grinding machine. 1: headstock, 2: grinding wheel, 3: wheel head, 4: tailstock, 5: worktable, 6: center rest, and 7: crankshaft.

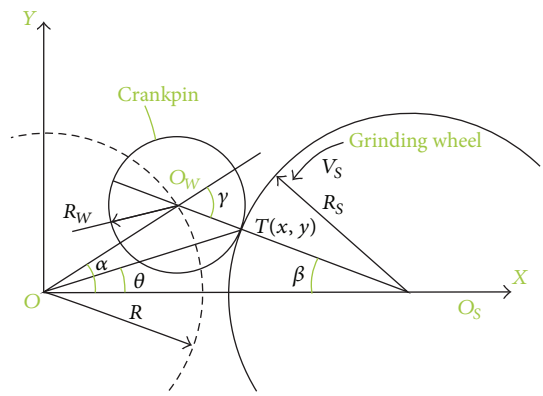

Figure 3: Crankshaft Tangential Point Tracing grinding movement schematic diagram.

The movement equation of wheel center O_S is as follows:

$$X = \overline{OO_S} = R\cos\alpha + (R_S + R_W)\cos\beta. \tag{2}$$

3. The Dynamic Model of Tangential Point Tracing Grinding System

3.1. Modeling and Formulation. The crankshaft is supported by the centers of the headstock and tailstock when it is machining. In order to reduce the deformation, main journals are supported by center rests. The headstock provides the low speed rotational drive to the crankshaft.

The crankpin moves around O point in the XOY plane while the grinding wheel is doing a reciprocating movement in X direction as shown in Figures 3 and 4(a). In this study, a simplified dynamic model of Tangential Point Tracing grinding machine and analysis are presented in Figure 4(c).

According to Newton motion law, four discrete mass dynamic equations are written as follows:

$$\begin{aligned} k_2(q_3 - q_1) - c_1\dot{q}_1 - k_1 q_1 &= m_1\ddot{q}_1 \\ Q_1 - k_2(q_3 - q_1) - c_3\dot{q}_3 - k_3 q_3 &= m_2\ddot{q}_3 \\ k_a(-q_2) - c_4\dot{q}_2 - k_4 q_2 &= m_1\ddot{q}_2 \\ Q_2 - k_a(-q_2) &= 0 \end{aligned} \tag{3a}$$

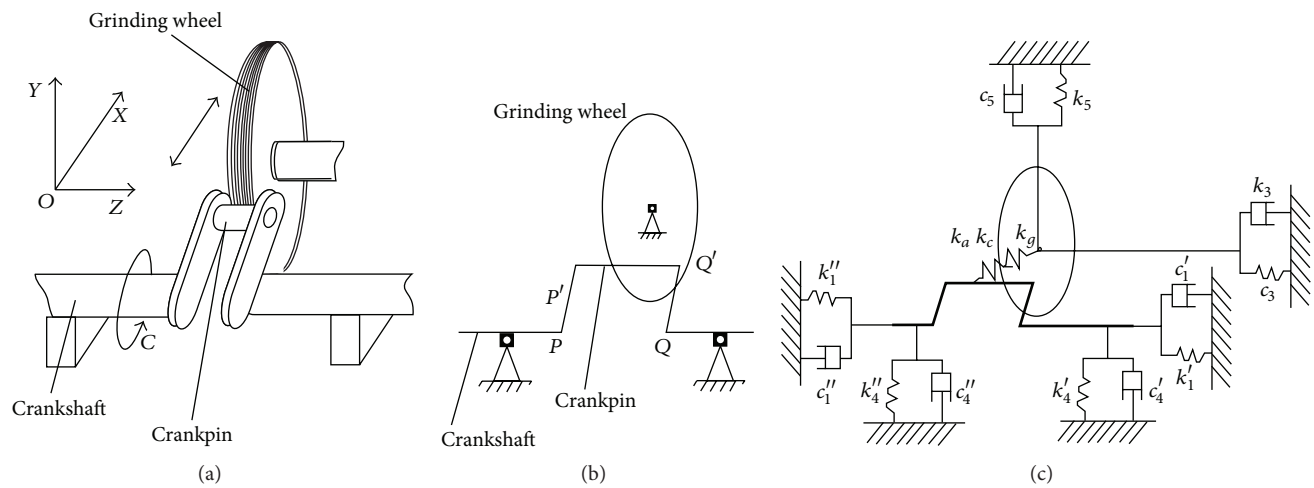

Figure 4: A simplified dynamic model of Tangential Point Tracing grinding machine.

$$\begin{aligned} m_1\ddot{q}_1 + c_1\dot{q}_1 + (k_1 + k_2)\, q_1 - k_2 q_3 &= 0 \\ m_2\ddot{q}_3 + c_3\dot{q}_3 + (k_2 + k_3)\, q_3 - k_2 q_1 &= Q_1 \\ m_1\ddot{q}_2 + c_4\dot{q}_2 + (k_4 + k_a)\, q_2 &= 0 \\ k_a(-q_2) &= Q_2. \end{aligned} \tag{3b}$$

For computer analysis and calculation, the upper type is changed into matrix form; the mass matrix of the system is as follows:

$$[m] = \begin{bmatrix} m_1 & 0 & 0 & 0 \\ 0 & m_2 & 0 & 0 \\ 0 & 0 & m_1 & 0 \\ 0 & 0 & 0 & m_2 \end{bmatrix}. \tag{4}$$

Damping matrix is

$$[c] = \begin{bmatrix} c_1 & 0 & 0 & 0 \\ 0 & c_2 & 0 & 0 \\ 0 & 0 & c_3 & 0 \\ 0 & 0 & 0 & c_4 \end{bmatrix}. \tag{5}$$

Stiffness matrix is

$$[k] = \begin{bmatrix} k_1 + k_2 & -k_2 & 0 & 0 \\ -k_2 & k_2 + k_3 & 0 & 0 \\ 0 & 0 & k_4 + k_a & -k_a \\ 0 & 0 & -k_a & k_a + k_5 \end{bmatrix}. \tag{6}$$

The generalized coordinates and generalized forces are expressed as

$$\{q\} = \{q_1 \;\; q_2 \;\; q_3 \;\; 0\}^T \tag{7a}$$

$$\{Q\} = \{0 \;\; Q_1 \;\; 0 \;\; Q_2\}^T. \tag{7b}$$

And we can express the above kinetic equation as

$$[m]\{\ddot{q}\} + [c]\{\dot{q}\} + [k]\{q\} = \{Q\}. \tag{8}$$

3.2. The Crankshaft Stiffness Is Different in the Circumferential Direction. The stiffness of the crankshaft varies not only along the axial direction, but also in the radial direction. It leads to the crankpin deformation in the circumferential direction and affects accuracy of the crankpin. In the cylindrical grinding, the direction of the normal grinding force (F_n) and the tangential grinding force (F_t) is invariable, but they change in the Tangential Point Tracing grinding. The grinding force is shown in Figure 5 where the angle of the crankpin is α:

$$\begin{aligned} F_U &= -F_n \times \cos\varphi - F_t \times \sin\varphi \\ F_V &= F_n \times \sin\varphi - F_t \times \cos\varphi \\ M &= -F_t \times R_W. \end{aligned} \tag{9}$$

The relationship between normal grinding force and tangential grinding force can be written as follows:

$$F_t = \zeta \times F_n. \tag{10}$$

4. Calculation of Critical Grinding Depth

Adjustment of the grinding process and modification of the machine tools structure are two approaches to avoid chatter. In the first approach, the stability lobe diagram that predicts the onset of chatter is used to determine the critical grinding depth and spindle speed to eliminate or minimize chatter behavior in machining [10].

It is important to study chatter mechanisms to predict critical grinding depth. We need to know grinding chatter boundaries and growth rates, which is helpful to design a grinding process without chatter according to the chatter boundaries.

In order to simplify the model of crankshaft cut into grinding system, the kinematic differential equation of the grinding wheel workpiece grinding system dynamics model is expressed as [11]

$$m\ddot{q}(t) + c\dot{q}(t) + kq(t) = \pm F(t). \tag{11}$$

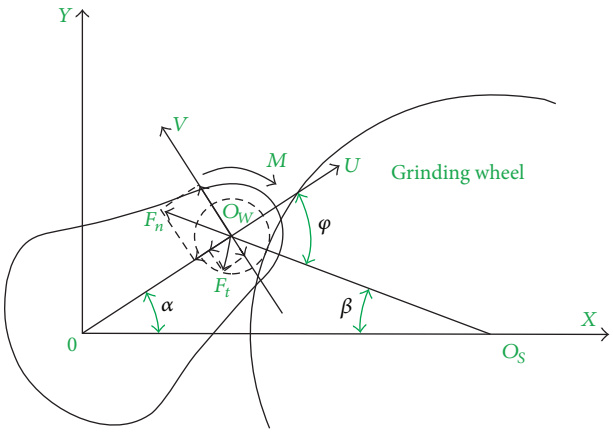

FIGURE 5: Schematic diagram of grinding force decomposition.

Dynamic grinding force is usually proportional to the removal rate of material, which has the following formula:

$$F(t) = \pm k'_m hba(t). \tag{12a}$$

Among them $a(t)$ are t moments of the surface of the workpiece (or wheel) surface ripple amplitude. In this model, only the delay effect from the workpiece is considered. The delay time τ is assumed to be constant and equals the workpiece's rotation period (T) [12]:

$$a(t) = a_0(t) - [q(t) - q(t-T)]. \tag{12b}$$

And then

$$F(t) = \pm k'_m hb\{a_0(t) - [q(t) - q(t-T)]\}. \tag{13}$$

After combining (11) and (13), we obtain the following expression:

$$\begin{aligned} &m\ddot{q}(t) + c\dot{q}(t) + kq(t) \\ &\quad = \pm k'_m hb\{a_0(t) - [q(t) - q(t-T)]\}. \end{aligned} \tag{14}$$

Laplace transformations to the upper formula can be

$$\begin{aligned} &\left(ms^2 + cs + k\right) q(s) \\ &\quad = k'_m hb\left[a_0(s) - q(s) + e^{-Ts} q(s)\right]. \end{aligned} \tag{15}$$

Then

$$\begin{aligned} &\left(ms^2 + cs + k\right) q(s) \\ &\quad = k'_m hb\left[-1 + e^{-Ts}\right] q(s) + k'_m hba_0(s) \\ &\left\{\left(ms^2 + cs + k\right) + k'_m hb\left[1 - e^{-Ts}\right]\right\} q(s) \\ &\quad = k'_m hba_0(s), \end{aligned} \tag{16}$$

where $q(s)$ is input and $a_0(s)$ is the output of the dynamic grinding process transfer function:

$$\frac{q(s)}{a_0(s)} = \frac{k'_m hb}{\left(ms^2 + cs + k\right) + k'_m hb\left(1 - e^{-Ts}\right)}. \tag{17}$$

Let

$$W(s) = \frac{1}{ms^2 + cs + k} \tag{18}$$

$$\frac{q(s)}{a_0(s)} = \frac{k'_m hbW(s)}{1 + k'_m hb\left(1 - e^{-Ts}\right) W(s)}. \tag{19}$$

To let the divisor be zero, the crankshaft (or wheel) system for the characteristic equation of regenerative chatter is

$$1 + k'_m hb\left(1 - e^{-Ts}\right) W(s) = 0. \tag{20}$$

According to the first discrimination method of stable Lyapunov system, $s = \sigma + i\omega$; the system is in the critical state of stability when σ is 0:

$$W(i\omega) = \frac{-1}{k'_m hb\left(1 - e^{-i\omega T}\right)}. \tag{21}$$

According to Euler equation, $e^{-i\omega T} = \cos(\omega T) - i\sin(\omega T)$ will be substituted into the above equation:

$$W(i\omega) = \frac{-1}{k'_m hb}\left\{\frac{1}{2} + \frac{-i\sin(\omega t)}{2[1 - \cos(\omega t)]}\right\}. \tag{22}$$

After rearranging (18), we obtain the following expression:

$$W(s) = \frac{1}{m\left(s^2 + (c/m)s + k/m\right)} \tag{23}$$

$$\omega_n{}^2 = \frac{k}{m} \tag{24}$$

$$\xi = \frac{-c}{2m\omega_n} \tag{25}$$

$$\lambda = \frac{\omega}{\omega_n}; \tag{26}$$

$s = i\omega$ will be substituted into (23):

$$\begin{aligned} W(s) &= \frac{1}{m\left(s^2 + (c/m)s + k/m\right)} \\ &= \frac{1}{m\omega_n{}^2}\left[\frac{1 - \lambda^2}{(1 - \lambda^2) + (2\xi\lambda)^2} - i\frac{2\xi\lambda}{(1 - \lambda^2) + (2\xi\lambda)^2}\right]. \end{aligned} \tag{27}$$

The real part of (21) and (27) is equal to

$$\frac{-1}{2k'_m hb} = \frac{1 - \lambda^2}{m\omega_n{}^2\left[(1 - \lambda^2) + (2\xi\lambda)^2\right]} \tag{28}$$

$$h = \frac{-m\omega_n{}^2\left[\left(1 - \lambda^2\right) + (2\xi\lambda)^2\right]}{2k'_m b\left(1 - \lambda^2\right)}. \tag{29}$$

To make (29) for a partial derivative of λ, then let the result approach zero:

$$\lambda = \sqrt{1 \pm 2\xi}. \tag{30}$$

Bring (30) into (29); then we get the critical grinding depth:

$$h_{\text{critical}} = \frac{2k\xi\,(1+\xi)}{k'_m b}. \tag{31}$$

It is shown that the presented approach can be used to predict the crankshaft grinding stability [5, 13].

The grinding wheel is easily worn and the regenerative chatter of both workpiece and grinding wheel should be considered.

Critical grinding depth of the crankshaft:

$$h_{\text{critical-}q} = \frac{2k_q\xi_q\left(1+\xi_q\right)}{k'_{mq} b}. \tag{32}$$

Critical depth of the grinding wheel wear:

$$h_{\text{critical-}s} = \frac{2k_s\xi_s\left(1+\xi_s\right)}{k'_{ms} b}. \tag{33}$$

5. Experimental Study

The complicated phenomena in engineering cannot be concluded only by theoretical analysis and the accuracy of theoretical analysis results need be verified by experiment.

5.1. The Test Experiment of Crankshaft Circumferential Stiffness Change. As the crankshaft is an elongate and complex shape shaft, the crankpin deforms during the grinding process. The center frame is generally used in the machining of crankshaft to eliminate the influence of the gravity, so the grinding force is the main cause of crankpin deformation.

In order to further study the influence of grinding force on the deformation of crankpin, we take the crankshaft of D06A-101-30 diesel engine as the experimental object. The number 1 crankpin was applied to the 200 N vertical constant force to simulate the idea that the crankshaft was stressed by the normal grinding force of 200 N. In the experiment, two laser displacement sensors were used to measure the deformation of crankpin in two directions, as shown in Figure 6.

First, the crankshaft is rotated without the weight, and the position of the crankpin is measured at 5 degrees from the angle of crankpin which is 0 degrees. Then, under the weight of 200 N, repeat the above measurement procedure and another group of position dates is obtained. The difference between the two groups is the deformation in the radius direction of crankpin under the grinding force 200 N. Finally we can achieve the deformation and stiffness of crankpin as in Table 1 and Figure 7:

$$K = \frac{P}{\Delta R}, \tag{34}$$

where K and P represent stiffness of crankpin and grinding force, respectively. ΔR denotes the deformation in the radius direction of crankpin.

According to the experimental results and the structural characteristics of the crankshaft, we use cosine curve fitting its stiffness, as shown in Figure 8. We can obtain the expression of the stiffness of the crankshaft.

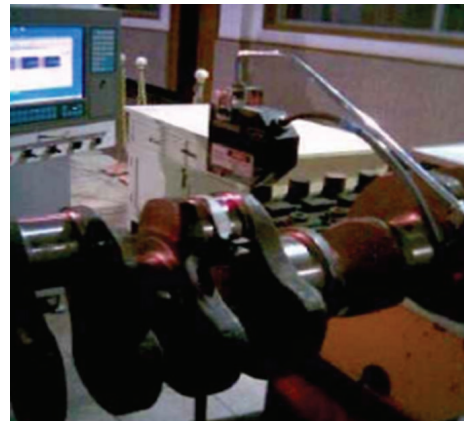

Figure 6: The test experiment of crankshaft circumferential stiffness.

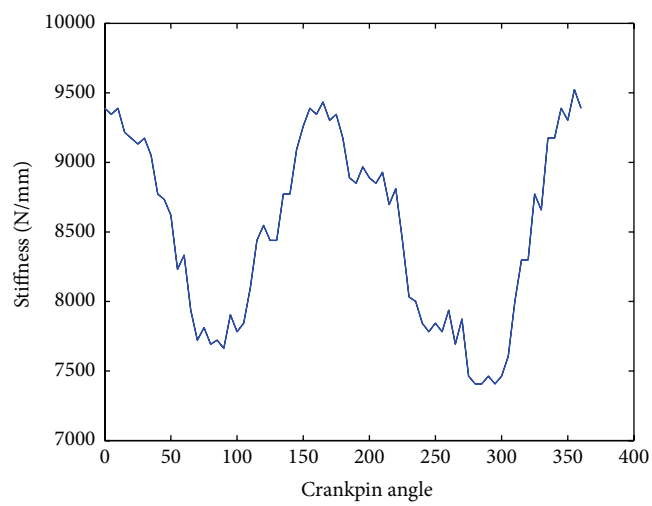

Figure 7: Crankpin Stiffness of the experiment.

If we plug the parameters of Table 2 into the above formulas, we can obtain the stability lobe diagram shown in Figure 9.

In the diagram, above the lobe line is "The unstable region" of the grinding system and below the lobe line is "The stability region."

The crankshaft is a complex shape shaft and its circumferential stiffness is different [14, 15]. In the diagram, it is shown that accounting for the uncertainty or variability of the process parameters can influence the stability boundary and the fuzzy stable region has been formed [16].

As the grinding wheel speed increasing, the limit grinding depth also has the tendency of increase. Therefore, by increasing the grinding wheel speed and keeping the grinding depth less than the critical depth, we can make the process in a stable state and the processing efficiency is improved.

Table 1: The deformation and stiffness of crankpin.

The angle of crankpin (°)	The deformation (mm)	Stiffness of crankpin (N/mm)
0	0.0213	9389.671
5	0.0214	9375.934
10	0.0213	9389.671
15	0.0217	9216.590
20	0.0218	9174.312
25	0.0219	9132.420
30	0.0218	9174.312
35	0.0221	9049.774
40	0.0228	8771.930
45	0.0229	8733.624
50	0.0232	8620.690
55	0.0243	8230.453
60	0.0240	8333.333
65	0.0252	7936.508
70	0.0259	7722.008
75	0.0256	7812.500
80	0.0260	7692.308
85	0.0259	7722.008
90	0.0261	7662.835
95	0.0253	7905.138
100	0.0257	7782.101
105	0.0255	7843.137
110	0.0247	8097.166
115	0.0237	8438.819
120	0.0234	8547.009
125	0.0237	8438.819
130	0.0237	8438.819
135	0.0228	8771.930
140	0.0228	8771.930
145	0.0220	9090.909
150	0.0216	9259.259
155	0.0213	9389.671
160	0.0214	9375.934
165	0.0212	9433.962
170	0.0215	9302.326
175	0.0214	9375.934
180	0.0218	9174.312
185	0.0225	8888.889
190	0.0226	8849.558
195	0.0223	8968.610
200	0.0225	8888.889
205	0.0226	8849.558
210	0.0224	8928.571
215	0.0230	8695.652
220	0.0227	8810.573
225	0.0237	8438.819
230	0.0249	8032.129
235	0.0250	8000.000
240	0.0255	7843.137
245	0.0257	7782.101
250	0.0255	7843.137
255	0.0257	7782.101
260	0.0252	7936.508
265	0.0260	7692.308
270	0.0254	7874.016
275	0.0268	7462.687
280	0.0270	7407.407
285	0.0270	7407.407
290	0.0268	7462.687
295	0.0270	7407.407
300	0.0268	7462.687
305	0.0263	7604.563
310	0.0250	8000.000
315	0.0241	8298.755
320	0.0241	8298.755
325	0.0228	8771.930
330	0.0231	8658.009
335	0.0218	9174.312
340	0.0218	9174.312
345	0.0213	9389.671
350	0.0215	9302.326
355	0.0210	9523.810
360	0.0213	9389.671

Table 2: The parameter of the grinding process.

k'_m (N/mm^2)	k (N/mm)	ξ	ω (rad/s)	b (mm)
1025	$(8.503903 + \cos\theta) * 1000$	0.053	439.82	30

5.2. Experimental Results Contrast. In order to verify the correctness of the stability limit diagram, we carried out the relevant grinding experiments [17–19]. The specific parameters of the workpiece and grinding wheel are shown in Table 3.

We apply Bruel & Kjaer 4366 accelerometer to the grinding machine in order to detect chatter vibrations. The sensor was mounted on the tailstock center (Figure 11). In the process of grinding, the acceleration amplitude of regenerative chatter is increased rapidly with the grinding time. Figures 12 and 13 display the normal and the chatter signals.

Crankshaft Tangential Point Tracing grinding setup is shown in Figure 10. Each test was measured more than three times during grinding, so that the signals produced were sufficient to obtain information.

Table 3: The specific parameters of the workpiece and grinding wheel.

Name of the workpiece	Material of the workpiece	Type of grinding wheel
Diesel engine crankshaft	CK45	AWA(19A)-white corundum mixed abrasive

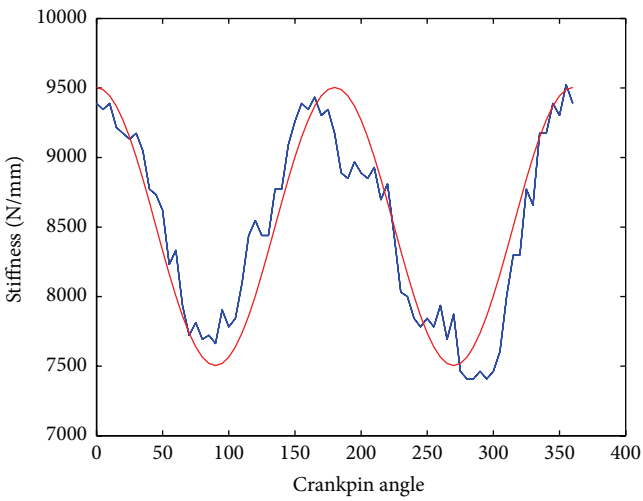

Figure 8: Crankpin Stiffness of the experiment and fitting curve.

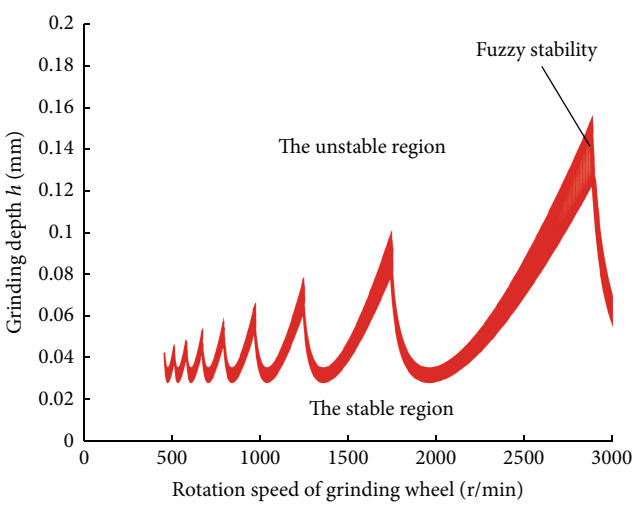

Figure 9: Stability lobe diagram.

The crankshaft rotation speed is set to 6 r/min and the speed of the grinding wheel is 1250 r/min, 1450 r/min, and 1650 r/min in grinding experiment. In the case of certain rotational speed, the boundary value of the chatter is determined continuously by changing the depth of the grinding. The chatter points are basically over the stability limit of the curve or near and so the experimental results are consistent with the predictions of the stability limit diagram. Therefore, it is proved that the prediction method is effective and reliable.

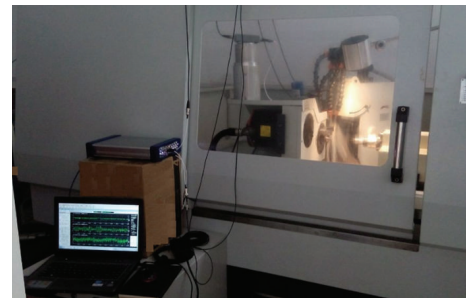

Figure 10: Experiment setup.

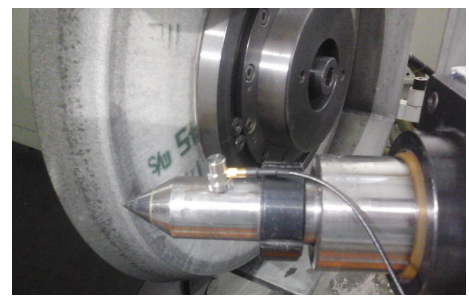

Figure 11: The position of acceleration sensors.

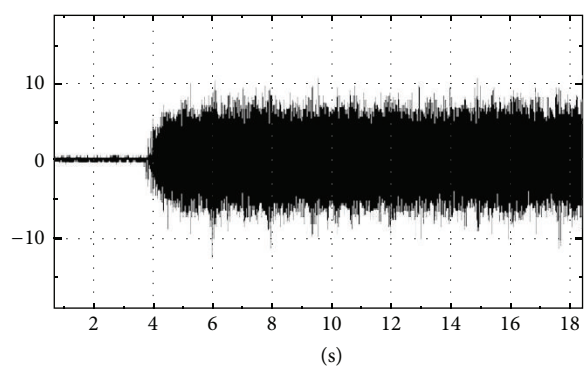

Figure 12: The normal signals.

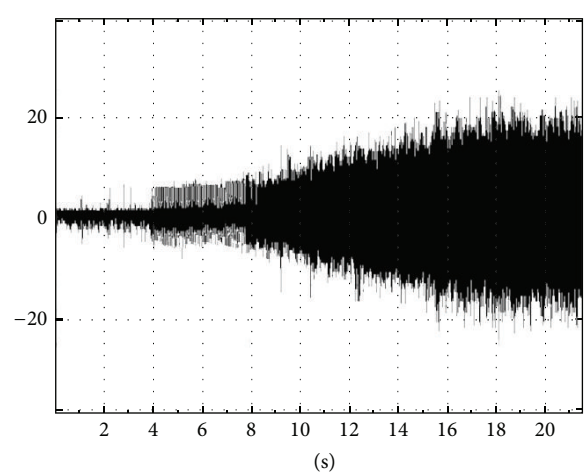

Figure 13: The chatter signals.

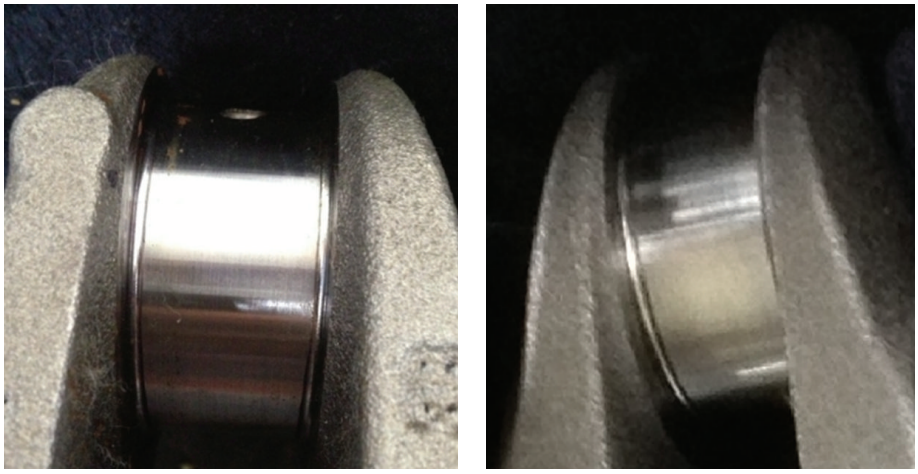

(a) Vibration Waviness of crankpin (b) Vibration Waviness of crankpin

Figure 14: Crankpin surface after chatter in grinding.

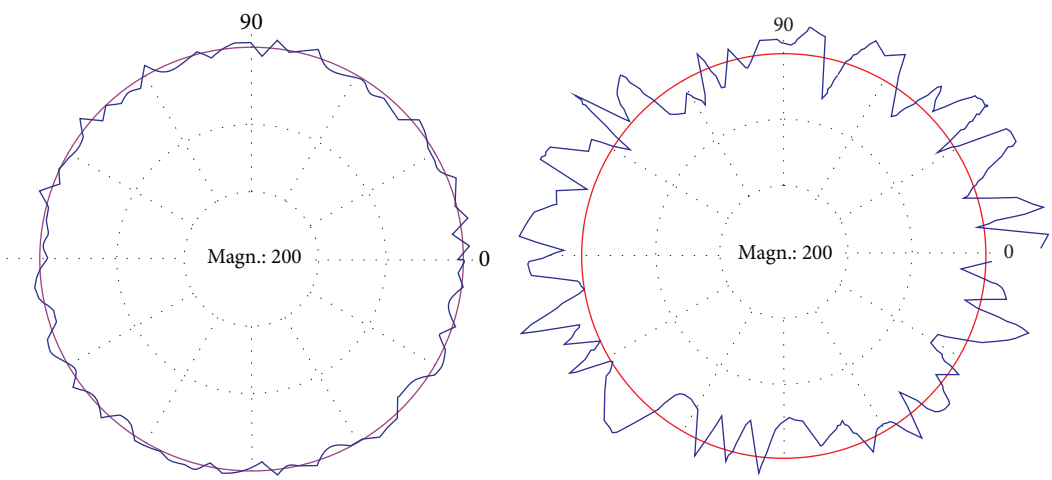

(a) The normal (b) The grinding chatter

Figure 15: The crankpin profile.

We can see chatter marks (Vibration Waviness) with naked eye on the crankpin surface as in Figure 14. Roundness measurement results show that the instability of the regenerative chatter caused by the instability of the grinding phenomenon makes the roundness of the workpiece poor, as shown in Figure 15.

6. Conclusions

To study how to avoid chatter in crankshaft Tangential Point Tracing grinding, Stability lobe diagram has been developed based on dynamic model to predict chatter and some conclusions have been drawn as follows:

(1) The dynamic equation of the grinding system has been constructed by the dynamic analysis of the grinding system.

(2) Expression of the critical crankshaft grinding depth has been developed based upon the work of Altintaş and Budak [5] and Stepan [13].

(3) Through the experimental study, the law of crankshaft rigidity is obtained.

(4) The stability of the grinding system can be predicted by using the method of drawing the stability diagram.

(5) Experimental results show that the prediction method is consistent with the experimental data.

Nomenclature

k_1 and k_4: Equivalent stiffness of the support system of X and Y direction in generalized coordinates in the time of the grinding of the crankpin, respectively

k_1' and k_4': Equivalent stiffness of the right support system of X and Y direction in generalized coordinates in the time of the grinding of the crankpin, respectively

k_1'' and k_4'': Equivalent stiffness of the left support system of X and Y direction in generalized coordinates in the time of the grinding of the crankpin, respectively: $k_1 = k_1' + k_1''$; $k_4 = k_4' + k_4''$

c_1 and c_4: Equivalent damping of the support system of X and Y direction in generalized coordinates in the time of the grinding of the crankpin, respectively

c_1' and c_4': Equivalent damping of the right support system of X and Y direction in generalized coordinates in the time of the grinding of the crankpin, respectively

c_1'' and c_4'': Equivalent damping of the left support system of X and Y direction in generalized coordinates in the time of the grinding of the crankpin, respectively: $c_1 = c_1' + c_1''$; $c_4 = c_4' + c_4''$

k_c: Contact stiffness of crankshaft and grinding wheel

k_g: Grinding rigidity of crankshaft and grinding wheel

k_a: Normal grinding stiffness of crankshaft and grinding wheel

k_2: The grinding stiffness and contact stiffness's equivalent stiffness of the crankshaft and the grinding wheel: $k_2 = k_c k_g/(k_c + k_g)$

k_3: Equivalent support stiffness of the grinding wheel system in the X direction of the generalized coordinates

c_3: The equivalent damping of the grinding wheel system in the X direction of the generalized coordinate system

m_1: Masses of the crankshaft

m_2: Masses of the grinding wheel

k_5: Equivalent stiffness of the support system of the grinding wheel of Y direction in generalized coordinates

c_5: Equivalent damping of the support system of the grinding wheel of Y direction in generalized coordinates

Q_1: The force of the grinding system in the direction of X of the generalized system

Q_2: The force of the grinding system in the direction of Y of the generalized system

q_1 and q_2: The displacement of the crankshaft horizontal and vertical direction shift

q_3: The displacement of wheel horizontal direction shift

α: The rotation angle of crankpin

β: The angle between $\overline{O_S O_W}$ and $\overline{OO_S}$ (Figure 3)

R: The eccentric distance of the crankpin

R_s: The radius of the grinding wheel

R_w: The radius of the crankpin

F_n: The normal grinding force

F_t: The tangential grinding force

M: The additional couple

ζ: The friction coefficient between the contact surface of the grinding wheel and the crankpin

$F(t)$: The dynamic grinding force

t: The time

h_g: The grinding depth of the workpiece

h_w: The grinding depth of the wheel

h_g and h_w: The opposite of its direction, assuming the grinding depth of the workpiece is a positive direction

k_m': The grinding force coefficient of workpiece (or grinding wheel)

h: The grinding depth of workpiece (or grinding wheel)

b: The grinding contact width

$a_0(t)$: The vibration pattern of the surface of the workpiece (or wheel) for the moment

T: The rotation period of workpiece (or wheel)

ω_n: The square of natural frequency for the system

ξ: The system equivalent damping

λ: The frequency ratio.

Conflict of Interests

The authors declare that there is no conflict of interests regarding the publication of this paper.

Acknowledgments

This work is supported by National Science and Technology Major Project of China under Grant no. 2009ZX04001-111. It is also supported by Key Scientific Research Projects of Jiujiang University under Grant no. 2013ZD08. The authors are grateful for the financial support and also would like to thank the anonymous reviewers and the editor for their comments and suggestions.

References

[1] A. Walsh, *Mathematical modelling of the crankshaft pin grinding process [Ph.D. thesis]*, Deakin University, Victoria, Australia, 2004.

[2] T. Fujiwara, S. Tsukamoto, and M. Miyagawa, "Analysis of the grinding mechanism with wheel head oscillating type CNC crankshaft pin grinder," *Key Engineering Materials*, vol. 291-292, pp. 163–168, 2005.

[3] M. Hitchiner and J. Webster, "Recent advaiuces in amshaft and crankshaft grinding," *Abrasives Magazine*, pp. 7–12, 2001.

[4] J. Tlusty and M. Polacek, "The stability of machine tool against self excited vibrations in machining," in *Proceedings of the ASME Production Engineering Research Conference*, pp. 465–474, Pittsburgh, Pa, USA, 1963.

[5] Y. Altintaş and E. Budak, "Analytical prediction of stability lobes in milling," *CIRP Annals—Manufacturing Technology*, vol. 44, no. 1, pp. 357–362, 1995.

[6] I. Inasaki, B. Karpuschewski, and H.-S. Lee, "Grinding chatter—origin and suppression," *CIRP Annals—Manufacturing Technology*, vol. 50, no. 2, pp. 515–534, 2001.

[7] G. Quintana, J. Ciurana, and D. Teixidor, "A new experimental methodology for identification of stability lobes diagram in milling operations," *International Journal of Machine Tools and Manufacture*, vol. 48, no. 15, pp. 1637–1645, 2008.

[8] K.-C. Cha, N.-Z. Wang, and J.-Y. Liao, "Dynamics and stability analysis of the simplified model for the surface grinder in various worktable positions," *Proceedings of the Institution of Mechanical Engineers Part K: Journal of Multi-Body Dynamics*, vol. 225, no. 3, pp. 220–234, 2011.

[9] R. Drazumeric, J. Badger, and P. Krajnik, "Geometric, kinematical and thermal analyses of non-round cylindrical grinding," *Journal of Materials Processing Technology*, vol. 214, no. 4, pp. 818–827, 2014.

[10] Q. Song, X. Ai, and W. Tang, "Prediction of simultaneous dynamic stability limit of time–variable parameters system in thin-walled workpiece high-speed milling processes," *International Journal of Advanced Manufacturing Technology*, vol. 55, no. 9–12, pp. 883–889, 2011.

[11] T. L. Schmitz and K. S. Smith, *Machining Dynamics: Frequency Response to Improved Productivity*, Springer, New York, NY, USA, 2009.

[12] L. Yuan, V.-M. Järvenpää, E. Keskinen, and M. Cotsaftis, "Simulation of roll grinding system dynamics with rotor equations and speed control," *Communications in Nonlinear Science and Numerical Simulation*, vol. 7, no. 3, pp. 95–106, 2002.

[13] G. Stepan, "Modelling non-linear regenerative effects in metal cutting," *Philosophical Transactions of the Royal Society*, vol. 359, no. 1781, pp. 739–757, 2001.

[14] Z. Zhou, H. Luo, D. Xu, Z. Sun, and H. Mi, "Analysis and compensation of stiffness-error of crankshaft in tangential point tracing grinding," *Chinese Journal of Mechanical Engineering*, vol. 39, no. 6, pp. 98–101, 2003 (Chinese).

[15] G. Wu, *Research on the key technique on noncircular crankshaft grinding [Ph.D. thesis]*, Shanghai University, Shanghai, China, 2011 (Chinese).

[16] N. D. Sims, G. Manson, and B. P. Mann, "Fuzzy stability analysis of regenerative chatter in milling," *Journal of Sound and Vibration*, vol. 329, no. 8, pp. 1025–1041, 2010.

[17] C. F. Yao, Q. C. Jin, X. C. Huang, D. X. Wu, J. X. Ren, and D. H. Zhang, "Research on surface integrity of grinding Inconel718," *International Journal of Advanced Manufacturing Technology*, vol. 65, no. 5–8, pp. 1019–1030, 2013.

[18] K. Wegener, H.-W. Hoffmeister, B. Karpuschewski, F. Kuster, W.-C. Hahmann, and M. Rabiey, "Conditioning and monitoring of grinding wheels," *CIRP Annals—Manufacturing Technology*, vol. 60, no. 2, pp. 757–777, 2011.

[19] G. Tlusty, *Manufacturing Processes and Equipment*, Prentice Hall, Upper Saddle River, NJ, USA, 2000.